AJNR

Diffusion MR Imaging Changes Associated with Wilson Disease

R.N. Sener

AJNR Am J Neuroradiol 2003, 24 (5) 965-967
http://www.ajnr.org/content/24/5/965

This information is current as of July 31, 2025.

AJNR Am J Neuroradiol 24:965–967, May 2003

Case Report

Diffusion MR Imaging Changes Associated with Wilson Disease

R.N. Sener

Summary: We herein report the case of a patient with Wilson disease. The patient underwent echo-planar diffusion MR imaging twice, 1.5 years apart. The lesions were in the putamina and caudate nuclei. At the first examination, undertaken after onset of extrapyramidal symptoms, a restricted diffusion pattern was evident. It is likely that this corresponded to cell swelling caused by the accumulation of copper. On the images obtained 1.5 years later, an opposite pattern (an elevated diffusion pattern) was noted. It is likely that this reflected necrosis, spongiform degeneration, and demyelination, which are among the known histopathologic changes associated with Wilson disease.

Neurologic symptoms of Wilson disease are usually caused by cerebral copper accumulation sufficient to destroy nerve cells. MR imaging findings in cases of Wilson disease have previously been described (1–8), and a few reports are available on MR spectroscopy (9) and diffusion MR imaging patients with this disease (10). We herein report a patient with Wilson disease who underwent two diffusion MR imaging studies performed 1.5 years apart.

Case Report

We report the case of an 11-year-old female patient with Wilson disease proved by liver biopsy. An MR imaging study was requested because she developed extrapyramidal symptoms. No sign of an acute ischemic condition was present. MR imaging was performed on a 1.5-T MR imaging unit. Maximum gradient strength was 30mT/m, and the rise time was 600 ms. Spin-echo T1- and T2-weighted sequences and diffusion-weighted MR images were obtained. A single shot, spin-echo, echo-planar sequence was used for diffusion MR imaging in the transverse imaging plane, indicated as "trace-0–500-1000-ADC." In this trace sequence, images with b = 50, b = 500, and b = 1000 s/mm^2 were obtained and apparent diffusion coefficient (ADC) maps were automatically generated. Images with b = 50 s/mm^2 were identical to those with b = 0 without gradient activation. Images with b = 500 and b = 1000 s/mm^2 were created by using averaged data with the x, y, and z gradients. Images with b = 1000 s/mm^2 corresponded to heavily diffusion-weighted images. The acquisition time was 22 s, with 5700/139 (TR/TE). The matrix was 96 × 128 mm, and the field of view was 240 mm. Each imaging set contained 20 sections with a section thickness of 5 mm.

Received June 11, 2002; accepted after revision September 16.

From the Department of Radiology, Ege University Hospital, Bornova, Izmir, 35100, Turkey.

Address reprint requests to Prof. Dr. R. Nuri Sener, Department of Radiology, Ege University Hospital, Bornova, Izmir, 35100, Turkey.

© American Society of Neuroradiology

Proton density– and T2-weighted images revealed symmetrical high signal intensity in the putamina and in the heads of the caudate nuclei, with an impression of some swelling of these nuclei. The globus pallidus appeared uninvolved (Fig 1A). The abnormal pattern on images with b = 1000 s/mm^2 consisted of high signal intensity changes (a restricted diffusion pattern similar to cytotoxic edema) in these regions (Fig 1B). On ADC maps, the corresponding regions revealed low signal intensity. ADC values were obtained by direct reading from the maps by using electronic evaluations (with pixel lens cursors), each including 16 pixels. At the sites with lesions, the ADC values were low: 0.49, 0.47, and 0.54 × 10^{-3} mm^2/s. For comparison, a normal ADC value from an unaffected parenchymal region was 0.82 × 10^{-3} mm^2/s (Fig 1C). Penicillamine therapy was started.

The patient was reexamined 1.5 years later. Extrapyramidal symptoms were persistent and were more severe despite the penicillamine therapy. The same MR imaging unit was used with the same imaging protocol. On T2-weighted images, it was noted that diffuse atrophy had developed and that the basal ganglion lesions had a different character with bilateral linear high signal intensity in the lateral putamen, intermixed high and low signal intensity changes in the medial region of the putamen, and high signal intensity in the caudate nucleus (Fig 2A). Heavily diffusion-weighted (b = 1000 s/mm^2) images had an appearance opposite that of the initial images with low signal intensity in the putamina and caudate nuclei (Fig 2B). ADC maps showed that the putaminal lesions had high signal intensity with a high ADC value: 2.08 × 10^{-3} mm^2/s, compared with that of normal parenchyma: 0.85 × 10^{-3} mm^2/s. Some parts of medial putamen had a very high ADC value, 6.01 × 10^{-3} mm^2/s, compared with that of normal CSF, 3.50 × 10^{-3} mm^2/s (Fig 2C). These were consistent with increased mobility of water molecules (elevated diffusion) as compared with the initial examination. Thus, these changes in the two diffusion MR imaging examinations performed 1.5 years apart likely corresponded to different stages of histopathologic changes in Wilson disease.

Discussion

In Wilson disease, ceruloplasmin, the serum transport protein for copper, is deficient. Copper is accumulated in the liver, and after hepatic binding sites are saturated, it is released. Systemic disease then develops.

The brain lesions are usually bilateral and often symmetrical, involving the putamen, caudate nucleus, globus pallidus, claustrum, thalamus, cortical/subcortical regions, mesencephalon, pons, vermis, and dentate nucleus. Histopathologic changes at these regions include edema, necrosis, and spongiform degeneration. These have been attributed to cellular damage caused by accumulation of copper, chronic ischemia, vasculopathy, or demyelination (1–10). The lesions of cerebral Wilson disease usually appear hyperintense on T2-weighted MR images (1–10). For

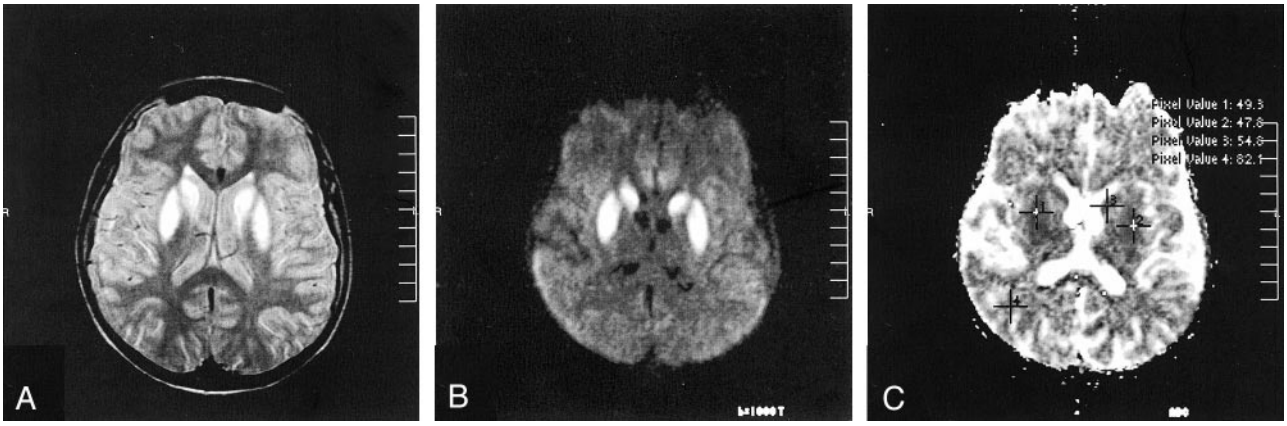

FIG 1. Images from initial examination.

A, Proton density–weighted image reveals bilateral high signal intensity in the putamina and in the heads of the caudate nuclei.

B, Heavily diffusion-weighted (b = 1000 s/mm^2) image reveals high signal intensity changes (restricted diffusion). This probably reflects accumulated copper.

C, Corresponding ADC map shows low ADC values, 0.49, 0.47, and 0.54 $\times$ 10^{-3} mm^2/s, in the corresponding regions, compared with a normal ADC value from the parenchyma, 0.82 $\times$ 10^{-3} mm^2/s.

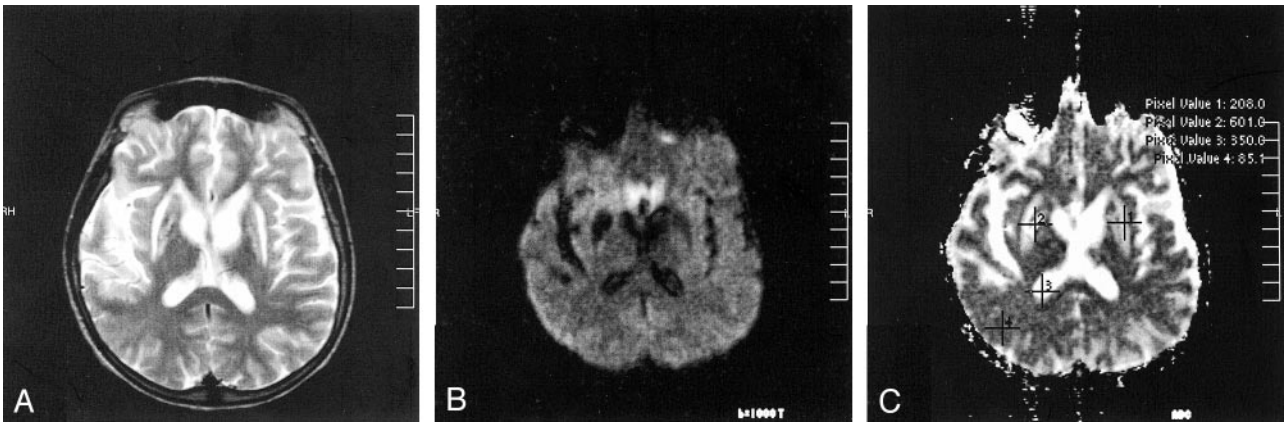

FIG 2. Images from second examination, performed 1.5 years later.

A, T2-weighted image reveals linear lesions in the putamina. Atrophy is noted.

B, Image with b = 1000 s/mm^2 reveals low signal intensity in the putamina.

C, Corresponding ADC map reveals high ADC values, 2.08 and 6.01 $\times$ 10^{-3} mm^2/s, in the putamina, compared with normal ADC value from the parenchyma, 0.85 $\times$ 10^{-3} mm^2/s. The ADC value of CSF is 3.50 $\times$ 10^{-3} mm^2/s.

our patient, the initial MR imaging study was obtained after recent onset of extrapyramidal symptoms, and the changes on T2-weighted images in the putamina and caudate nuclei consisted of diffuse high signal intensity with some swelling (Fig 1). This proceeded to linear high signal intensity changes and disappearance of swelling in 1.5 years (Fig 2). Also, diffuse cerebral atrophy developed during this period.

A study by Kishibayashi et al (10) dealt with diffusion MR imaging in cases of Wilson disease. They studied four patients and noted that there were abnormal high signals in some areas of the basal ganglia in each case (on heavily diffusion-weighted images) (10). The initial diffusion imaging pattern on the images of our patient consisted of high signal intensity lesions on heavily diffusion-weighted (b = 1000 s/mm^2) images, and an impression swelling of the putamina and caudate nuclei was present. Furthermore, ADC value measurements were available from automatically generated ADC maps. These revealed abnormally low ADC values, 0.49, 0.47, and 0.54 $\times$ 10^{-3} mm^2/s, compared with that of normal parenchymal value, 0.82 $\times$ 10^{-3} mm^2/s. It is known that such findings on diffusion MR images usually correspond to a restriction of mobility of water molecules and indicates the presence of cytotoxic edema (acute ischemia and infarct). In the case reported herein, however, such a mechanism was unlikely. Therefore, considering that excess copper causes cell injury leading to inflammation and cell death, it is likely that this finding mainly represented cell swelling associated with inflammation, hence restriction of diffusion (Fig 1).

With respect to the changes at the 1.5-year follow-up examination, there were low signals in the putamina and caudate nuclei on images with b = 1000 s/mm^2, and ADC maps revealed high signal intensity and high ADC values, 2.08, 6.01 $\times$ 10^{-3} mm^2/s, compared with those of normal parenchyma, 0.85 $\times$ 10^{-3} mm^2/s (Fig 2). These changes, which are consistent with increased mobility of water molecules (elevated diffusion) were opposite the findings of the initial examination. Considering the known histopathologic

changes associated with Wilson disease, it is likely that these reflected necrosis, spongiform degeneration, and demyelination in the stage of the disease at the 1.5-year follow-up study. The findings in this patient with Wilson disease suggested that diffusion MR imaging can provide data regarding different histopathologic stages of Wilson disease, and further studies should investigate this in detail.

References

1. Starosta-Rubinstein S, Young AB, Kluin K, et al. **Clinical assessment of 31 patients with Wilson's disease: correlations with structural changes on magnetic resonance imaging.** *Arch Neurol* 1987; 44:365–370
2. Aisen AM, Martel W, Gabrielsen TO, et al. **Wilson disease of the brain: MR imaging.** *Radiology* 1985;157:137–141
3. Uchino A, Maeoka N, Ohno M, Miyoshi T. **MR imaging of the brain in Wilson's disease [in Japanese].** *Rinsho Hoshasen* 1989;34: 1413–1416
4. Saatci I, Topcu M, Baltaoglu FF, et al. **Cranial MR findings in Wilson's disease.** *Acta Radiol* 1997;38:250–258
5. Sener RN. **The claustrum on MRI: normal anatomy, and the bright claustrum as a new sign in Wilson's disease.** *Pediatr Radiol* 1993; 23:594–596
6. Mochizuki H, Kamakura K, Masaki T, et al. **Atypical MRI features of Wilson's disease: high signal in globus pallidus on T1-weighted images.** *Neuroradiology* 1997;39:171–174
7. Takahashi W, Yoshii F, Shinohara Y. **Reversible magnetic resonance imaging lesions in Wilson's disease: clinical-anatomical correlation.** *J Neuroimaging* 1996;6:246–248
8. King AD, Walshe JM, Kendall BE, et al. **Cranial MR imaging in Wilson's disease**. *AJR Am J Roentgenol* 1996;167:1579–1584
9. Alanen A, Komu M, Penttinen M, Leino R. **Magnetic resonance imaging and proton MR spectroscopy in Wilson's disease.** *Br J Radiol* 1999;72:749–756
10. Kishibayashi J, Segawa F, Kamada K, Sunohara N. **Study of diffusion weighted magnetic resonance imaging in Wilson's disease [in Japanese].** *Rinsho Shinkeigaku* 1993;33:1086–1089